Supplemental Data

Structural Polymorphism in Amyloids: New Insights from Studies with Y145Stop Prion Protein Fibrils

Eric M. Jones,[†] Bo Wu,[‡] Krystyna Surewicz,[†] Philippe S. Nadaud,[‡] Jonathan J. Helmus,[‡] Shugui Chen,[†] Christopher P. Jaroniec,[‡] and Witold K. Surewicz[†]

[†]*Department of Physiology and Biophysics, Case Western Reserve University, Cleveland, OH 44106*
[‡]*Department of Chemistry, The Ohio State University, Columbus, OH 43210*

Resonance assignments of fragment K106-N108 in Δ113-120 PrP23-144 amyloid fibrils

As noted in the main text, assignments of the three-residue fragment, K106-N108, were complicated by significantly attenuated resonance intensities due to protein dynamics and are therefore somewhat tentative. While these assignments are not critical to the main conclusions of the paper, the rationale for them is briefly presented here along with possible alternatives. Focusing on this fragment, which clearly corresponds to three consecutive residues in the protein sequence, we immediately note that the spin system for the central amino acid is characteristic of a threonine with its highly distinctive pattern of ^{13}C chemical shifts (C^{α} = 58.0 ppm, C^{β} = 69.6 ppm, C^{γ} = 22.2 ppm). The fact that there are only three threonines in the entire Δ113-120 PrP23-144 sequence (T33, T95 and T107) initially yields three possible assignments for this fragment corresponding to aa 32-34 (NTG), 94-96 (GTH) and 106-108 (KTN). However, since the residue following threonine shows a clear $^{13}C^{\beta}$ signal in multiple NMR spectra (Fig. S3), this fragment cannot possibly correspond to NTG, leaving GTH and KTN as the two viable assignments.

Resolving the remaining two-fold ambiguity in the assignment based solely on the available experimental chemical shift data is rather difficult. For example, the residue following threonine has a $^{13}C^{\beta}$ chemical shift of 23.6 ppm, which is unusually low for asparagine even with secondary shift effects taken into account (according to the BioMagResBank database (1) the average chemical shift for asparagine C^{β} is ~38.7 ± 1.7 ppm with the full range of shifts reported in the database between ~29 and 55 ppm). Thus, considered on its own, this would argue in favor of the residue likely being a histidine (average C^{β} shift of ~30.2 ± 2.1 ppm with the full range of ~19-43 ppm in the BioMagResBank) belonging to the GTH fragment (aa 94-96). However, at the same time the residue preceding threonine displays an amide ^{15}N shift of ~118 ppm, which, although feasible, is unusual for glycines. Additionally, basing the entire assignment of a larger

protein fragment on a single C^{β} secondary shift with no other data connecting the fragment to any other residue would be highly speculative. Unfortunately, no other such data are available that can be used to resolve the ambiguity due to low spectral intensities for residues in this region of the protein. For instance, no $^{13}C^{\beta}$-$^{13}C^{\gamma}$ or ^{15}N-$^{13}C^{\gamma}$ correlations, which would readily distinguish between histidine and asparagine side-chains, are observed for the residues of interest in ^{13}C-^{13}C and ^{15}N-$^{13}C^{\alpha}$-^{13}CX spectra, respectively. Likewise, the identity of the residue preceding threonine in this three-residue fragment cannot be established with certainty—while relatively weak $^{13}C^{\alpha}$ and $^{13}C'$ signals are detected in the spectra with shifts compatible with both glycine and lysine residues, it is not absolutely clear whether the lack of any correlations involving $^{13}C^{\beta}$ is due to this amino acid being a glycine or simply a result of severely attenuated signal intensities.

In summary, the current assignment of the three-residue fragment above as K106-T107-N108 is based on a correlation between the ^{15}N of residue M109 and $^{13}C^{\alpha}$ of the preceding residue in the 3D NCOCX spectrum (Fig. S1 and Fig. S3), which connects the fragment to the rest of the protein sequence, combined with the fact that this three-residue segment directly borders the relatively rigid amyloid core region. Although, it remains somewhat tentative, in order to provide an additional measure of confidence in this assignment we have carried out an independent analysis of all the spectra using a Monte Carlo/simulated annealing automatic assignment program (2,3) kindly made available to us by Drs. Robert Tycko and Kan-Nian Hu. This analysis associates the correlations in question as indeed belonging to residues K106-N108, and furthermore confirms all the remaining chemical shift assignments reported herein for [Δ113-120] fibrils.

Table S1. ^{15}N and ^{13}C chemical shifts for residues in the amyloid core region of Δ113-120 PrP23-144 fibrils.

Residue	N	C′	Cα	Cβ	Cγ	Cδ
K106	118.1	172.2	49.4			
T107	108.5	170.7	58.0	69.6	22.2	
N108	121.9	175.0	49.8	23.6		
M109	121.4	174.3	53.6	35.2		
K110	125.1	174.0	54.2	35.3		
H111	121.6	174.1	51.3	35.5		
M112	122.2	173.5	53.8	36.1	34.0	
V121	127.2	173.8	60.4	35.6	22.3	
					19.9	
V122	129.3	174.1	60.3	32.8	21.9	
					21.0	
G123	113.6	173.3	44.1			
G124	107.8	172.4	44.9			
L125	124.3	177.3	55.1	38.8	28.2	27.6
						26.1
G126	112.2	175.6	47.2			
G127	113.5	170.3	48.9			
Y128	128.9	174.6	56.4	44.1		
M129	124.0	172.3	54.0	39.9	30.6	
L130	120.7	175.1	55.0	41.3	27.9	27.2
G131	107.5	173.3	47.6			
S132	122.5	174.5	55.8	63.1		
A133	123.4	175.7	52.5	20.8		
M134	118.4	174.4	53.9			
S135	118.9	173.6	55.2	64.8		
R136	128.1	170.9	53.1	31.0		
P137	134.6	175.8	61.9	33.4	27.2	48.8
I138	122.3	174.4	60.8	40.0	27.6	13.5
					16.9	
I139	126.7	174.3	59.8	40.6	28.3	15.2
					18.3	
H140	127.4	172.6	52.4			
F141	118.6	180.2	56.3	40.0		

Chemical shifts are reported in ppm and referenced relative to DSS using adamantane as a secondary standard, with the ^{13}C chemical shift of 40.48 ppm for the downfield resonance according to Morcombe and Zilm (4).

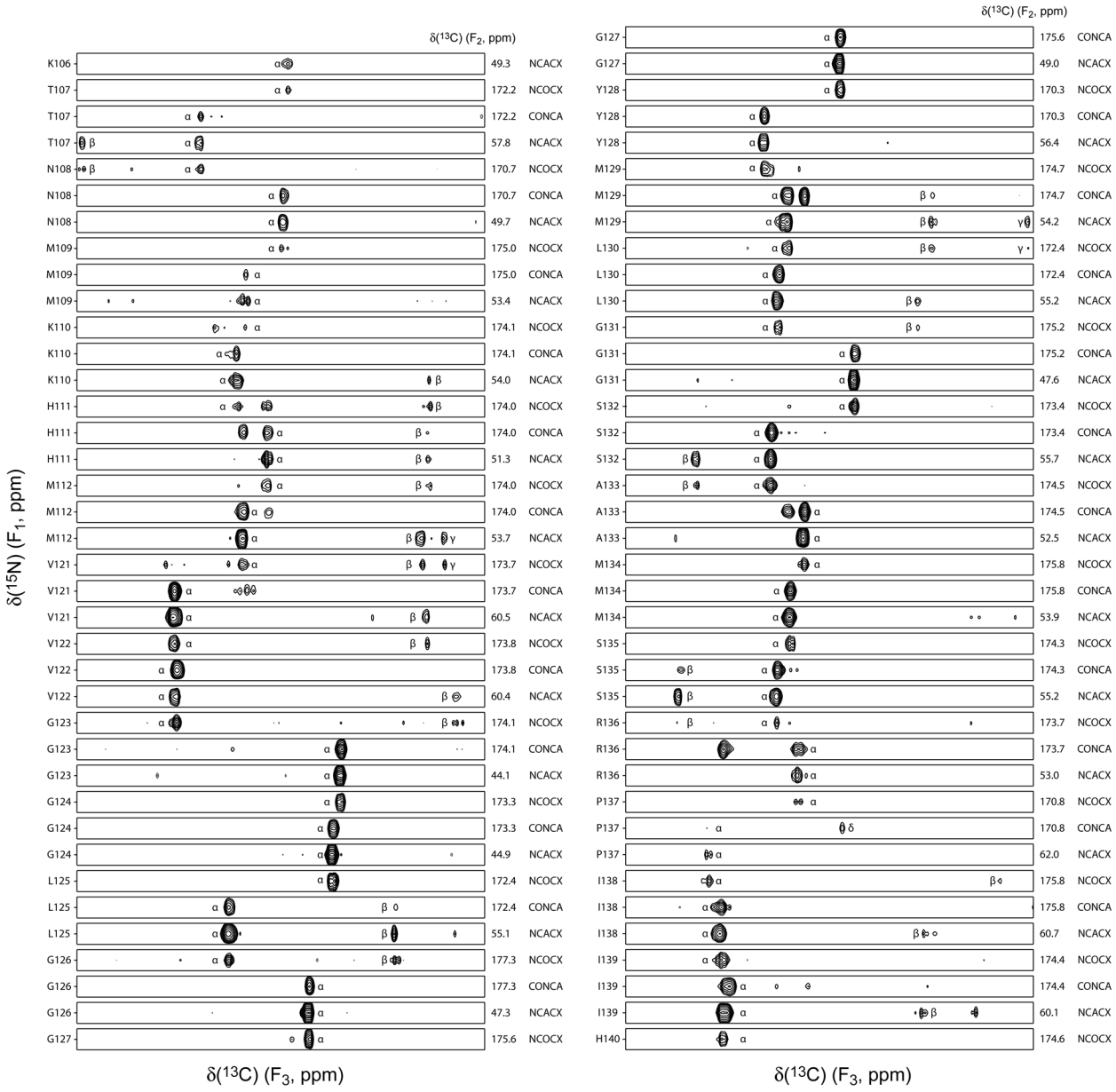

Fig. S1. Strips from 3D $^{13}C'$-^{15}N-$^{13}C^{\alpha}$ (CONCA), ^{15}N-$^{13}C^{\alpha}$-^{13}CX (NCACX), and ^{15}N-$^{13}C'$-^{13}CX (NCOCX) spectra for Δ113-120 PrP23-144 amyloid fibrils showing sequential backbone connectivity. Spectra were recorded at 11.7 T, 11.111 kHz MAS rate and effective sample temperature of ~5 ^{o}C, with pulse sequences and experimental parameters identical to those used previously for [WT] fibrils (5). Strips are labeled by residue number according to the ^{15}N frequency (F_1), with the ^{13}C frequencies (F_2) indicated to the right of each strip. Major cross-peaks corresponding to the appropriate α, β, γ and δ carbons are labeled.

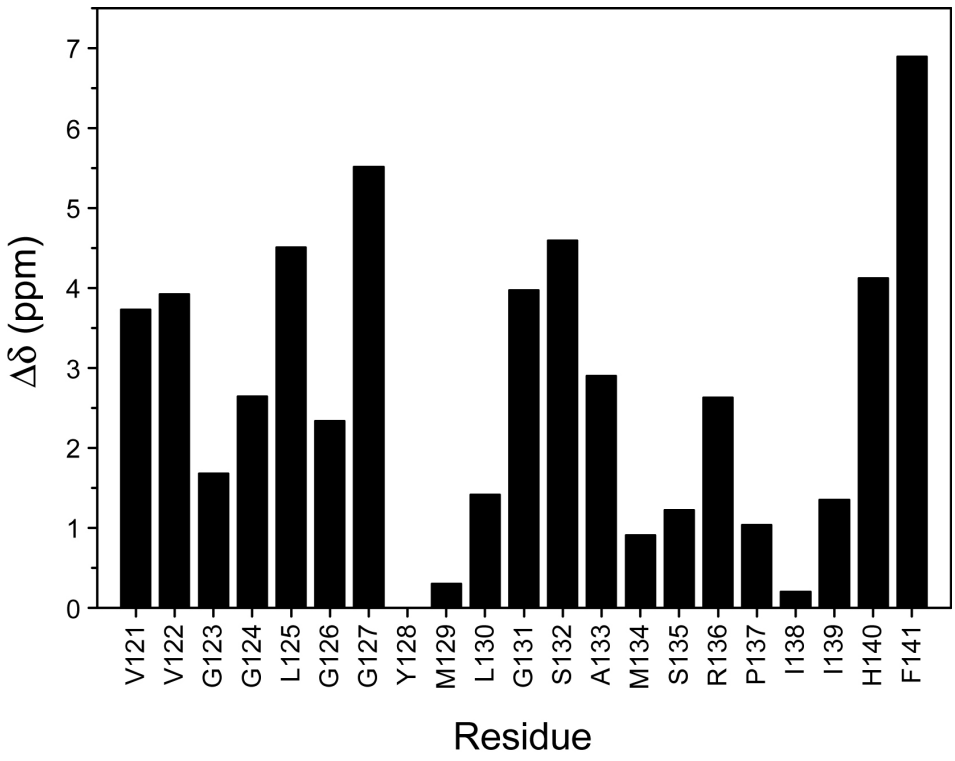

Fig. S2. Overall ^{13}C chemical shift changes, $\Delta\delta$, for residues V121-F141 in WT and Δ113-120 PrP23-144 amyloid fibrils ($\Delta\delta = \sqrt{(\Delta\delta_{CO})^2 + (\Delta\delta_{CA})^2 + (\Delta\delta_{CB})^2}$, where $\Delta\delta_{CO}$, $\Delta\delta_{CA}$, and $\Delta\delta_{CB}$ are the differences between $^{13}C'$, $^{13}C^{\alpha}$ and $^{13}C^{\beta}$ shifts, respectively, for [WT] and [Δ113-120] fibrils). The $\Delta\delta$ values range from ~0.2 ppm to ~7 ppm, with the average $\Delta\delta$ of 2.8 ± 1.8 ppm.

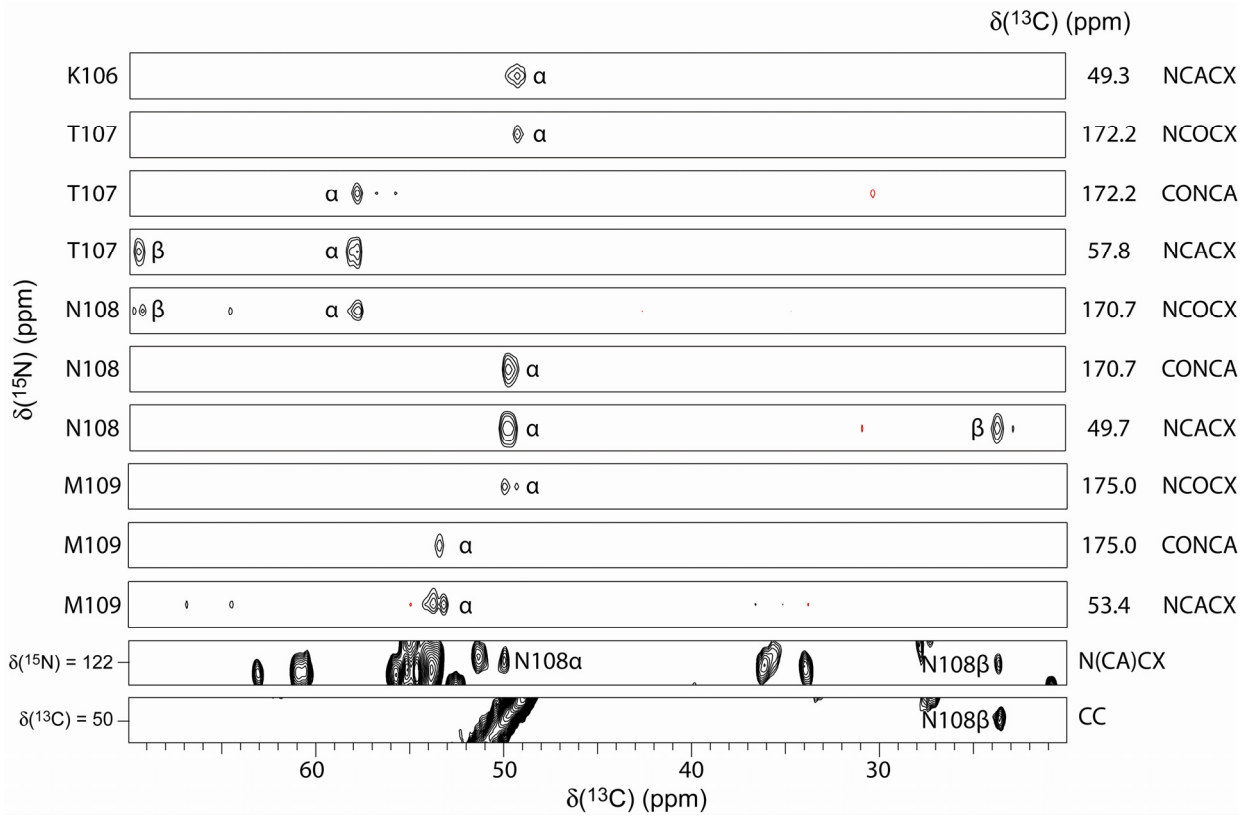

Fig. S3. Small regions of 2D and 3D solid-state NMR spectra used to establish the assignments of residues K106-N108 in [Δ113-120] amyloid fibrils as discussed in detail in the Supplemental Data text.

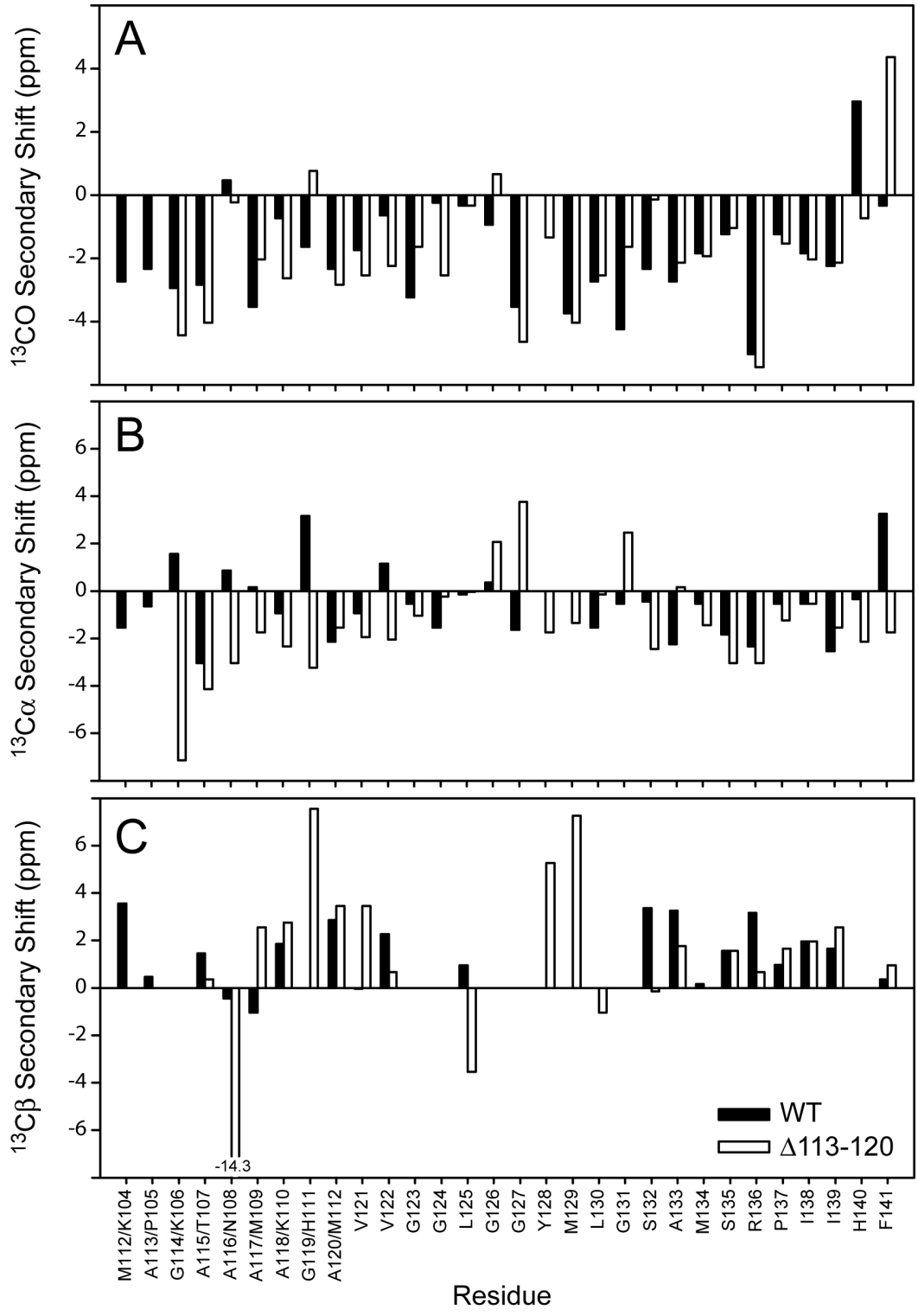

Fig. S4. $^{13}C'$ (A), $^{13}C^{\alpha}$ (B) and $^{13}C^{\beta}$ (C) secondary chemical shifts for [WT] and [Δ113-120] fibrils. The secondary chemical shifts were calculated as differences between the experimental chemical shifts and the corresponding random-coil chemical shifts.

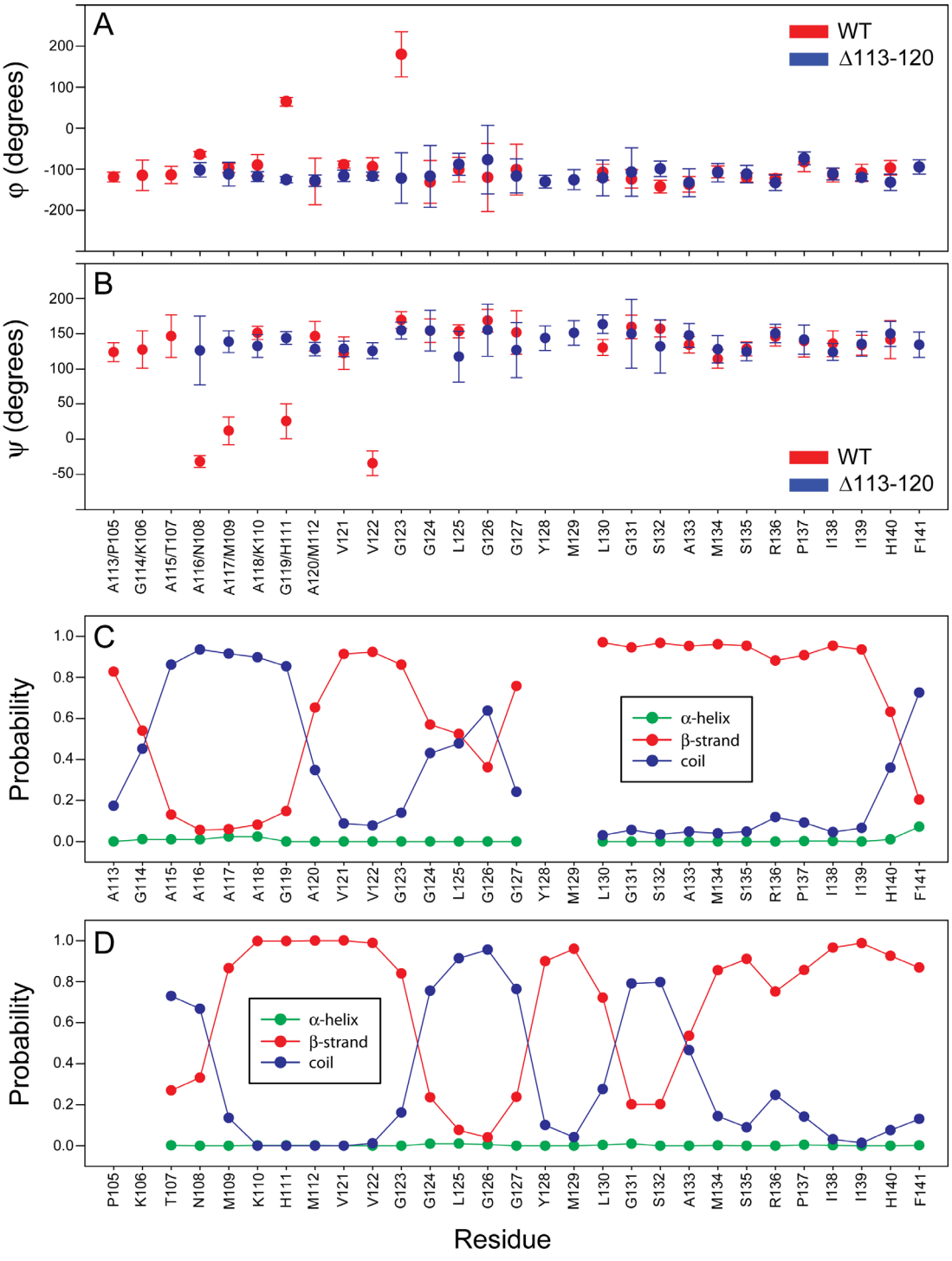

Fig. S5. TALOS+ (6) analysis of secondary structure in the core regions of [WT] and [Δ113-120] amyloid fibrils. (A,B) Predicted backbone φ (A) and ψ (B) torsion angles for [WT] fibrils (red) and [Δ113-120] fibrils (blue). Predicted φ and ψ values are reported only for those residues, for which at least 9 of 10 database hits were found in the same region of Ramachandran space. (C,D) Normalized probabilities of the different secondary structure types (α-helix, green circles; β-strand, red circles; coil, blue circles) for [WT] fibrils (C) and [Δ113-120] fibrils (D).

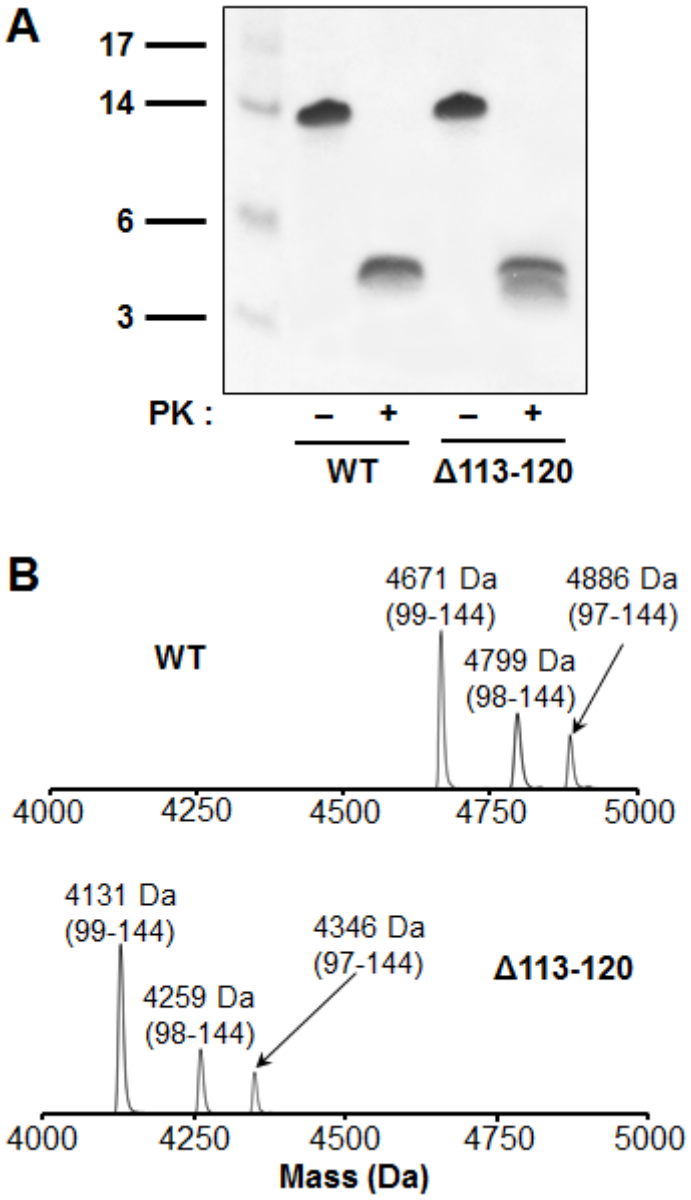

Fig. S6. Proteinase K resistance of WT and Δ113-120 PrP23-144 fibrils. (A) Coomasie blue stained SDS-PAGE gel. 20 mL aliquots of fibrils at 100 μM concentration were incubated for 30 min at 37 ^{o}C in the absence (-) or presence (+) of 1 μg/mL PK (Sigma) and then boiled for 10 min with 20 μL of 2x SDS-PAGE sample buffer. Aliquots (20 or 10 μL for PK-treated and non-treated samples, respectively) were applied on a 12% gel. (B) Mass spectra of fibrils after PK digestion. The numbers for each peak indicate the molecular mass and residues corresponding to matching PrP23-144 fragments. Spectra were acquired on a Thermo LTQ mass spectrometer.

References

1. Ulrich, E. L., Akutsu, H., Doreleijers, J. F., Harano, Y., Ioannidis, Y. E., Lin, J., Livny, M., Mading, S., Maziuk, D., Miller, Z., Nakatani, E., Schulte, C. F., Tolmie, D. E., Wenger, R. K., Yao, H., and Markley, J. L. (2008) *Nucleic Acids Res.* **36**, D402-D408
2. Tycko, R., and Hu, K. N. (2010) *J. Magn. Reson.* **205**, 304-314
3. Hu, K. N., Qiang, W., and Tycko, R. (2011) *J. Biomol. NMR* **50**, 267-276
4. Morcombe, C. R., and Zilm, K. W. (2003) *J. Magn. Reson.* **162**, 479-486
5. Helmus, J. J., Surewicz, K., Nadaud, P. S., Surewicz, W. K., and Jaroniec, C. P. (2008) *Proc. Natl. Acad. Sci. USA* **105**, 6284-6289
6. Shen, Y., Delaglio, F., Cornilescu, G., and Bax, A. (2009) *J. Biomol. NMR* **44**, 213-223